Journal of Reproduction and Development, Vol. 69, No 2, 2023

Original Article

A more accurate analysis of maternal effect genes by siRNA electroporation into mouse oocytes

Takuto YAMAMOTO[1)*], Shinnosuke HONDA[1)*], Issei IDEGUCHI[1)], Motoki SUEMATSU[1)], Shuntaro IKEDA[1)] and Naojiro MINAMI[1)]

[1)]*Laboratory of Reproductive Biology, Graduate School of Agriculture, Kyoto University, Kyoto 606-8502, Japan*

Abstract. Maternal RNA and proteins accumulate in mouse oocytes and regulate initial developmental stages. Sperm DNA combines with protamine, which is exchanged after fertilization with maternal histones, including H3.3; however, the effect of H3.3 on development post-fertilization remains unclear. Herein, we established an electroporation method to introduce H3.3 siRNA into germinal vesicle (GV)-stage oocytes without removing cumulus cells. Oocyte-attached cumulus cells need to be removed during the traditional microinjection method; however, we confirmed that artificially removing cumulus cells from oocytes reduced fertilization rates, and oocytes originally free of cumulus cells had reduced developmental competence. On introducing H3.3 siRNA at the GV stage, H3.3 was maintained in the maternal pronucleus and second polar body but not in the paternal pronucleus, resulting in embryonic lethality after fertilization. These findings indicate that H3.3 protein was not incorporated into the paternal pronucleus, as it was repeatedly translated and degraded over a relatively short period. Conversely, H3.3 protein incorporated into the maternal genome in the GV stage escaped degradation and remained in the maternal pronucleus after fertilization. This new method of electroporation into GV-stage oocytes without cumulus cell removal is not skill-intensive and is essential for the accurate analysis of maternal effect genes.

Key words: Electroporation, Germinal vesicle (GV)-stage oocytes, H3.3, Mouse, siRNA

(**J. Reprod. Dev. 69:** 118–124, 2023)

In mammals, maternal transcripts and proteins (maternal factors), known to support early embryonic development, accumulate during oogenesis. Given the minimal transcriptional activity that occurs during the development of fully grown oocytes to early one-cell embryos in mice [1–3], these transcripts and proteins are deemed to regulate the developmental program during and after this period. Some of these factors have already been shown to be involved in meiotic progression, maternal RNA degradation, and chromatin remodeling [4–6]. Typically, maternal transcripts undergo degradation around the two- to eight-cell stages in mice, coinciding with zygotic genome activation [7].

Knockout and transgenic mice are frequently employed to analyze the function of maternal factors [8–11]. However, these genetically modified techniques can be time-consuming and require the management of large numbers of animals. Subsequently, a method involving the direct microinjection of siRNA into germinal vesicle (GV)-stage oocytes or metaphase II (MII) oocytes was developed, facilitating the analysis of maternal factors in a single generation [12, 13]. Oocyte-attached cumulus cells need to be removed by pipetting before microinjection; however, the impact of this procedure on oocytes remains unclear. Electroporation was developed as an alternative gene delivery method and does not require skilled techniques such as microinjection [14]. Electroporation is frequently used to introduce Cas9-gRNA complexes, morpholino oligonucleotides, and plasmid DNAs into zygotes [14, 15]. In addition, an electroporation method to introduce siRNA into GV-stage oocytes has been established; however, this technique is markedly complicated, as it requires the removal of cumulus cells, thinning of the zona pellucida, and use of polyamine-based transfection reagents [16]. Two types of GV-stage oocytes can be artificially harvested from mouse ovaries: those surrounded by cumulus cells (cumulus-enclosed oocytes: CEOs) and those without associated cumulus cells (denuded oocytes: DOs) [3]. DOs exhibit a lower maturation rate and higher transcriptional activity than CEOs [17, 18]; however, the differences in subsequent fertilization and development rates between DOs, CEOs, and artificially denuded CEOs (dCEOs) remain poorly explored. Low numbers of cumulus cells surrounding oocytes have been associated with follicle atresia in humans, cynomolgus monkeys, cattle, and horses [19–22], which may explain the poor quality of DOs.

In mammals, three non-centromeric histone H3 variants (H3.1, H3.2, and H3.3) have been identified, and H3.3 is a known maternal factor. H3.3 is incorporated into the paternal pronucleus immediately after fertilization and promotes chromatin decondensation [13, 23–26]. H3.3 accumulates in active chromatin after the two-cell stage in mouse embryos and is considered to regulate embryo-specific gene expression patterns [27, 28]. Although several H3.3 knockdown experiments in MII- and GV-stage oocytes have been reported [13, 26, 29, 30], the post-fertilization developmental competence of H3.3-depleted GV-stage oocytes has not been examined.

In the present study, we investigated the differences in fertilization and development rates between DOs, CEOs, and dCEOs. CEOs exhibited higher fertility and developmental competence than DOs. Moreover, we observed that cumulus cells were essential for CEO fertility; hence, we developed a method that employed electroporation to introduce maternal transcript-targeting siRNAs into oocytes without cumulus cell removal. Using this electroporation method, we examined the function of H3.3 more precisely during embryonic

Received: November 10, 2022
Accepted: January 31, 2023
Advanced Epub: March 2, 2023

Correspondence: N Minami (e-mail: minami.naojirou.6r@kyoto-u.ac.jp)
* T Yamamoto and S Honda contributed equally to this work.

development after fertilization.

Materials and Methods

Collection of GV-stage oocytes

GV-stage oocytes were obtained from 8–12-week-old ICR mice (Japan SLC, Shizuoka, Japan) 48 h after injection with 7.5 IU equine chorionic gonadotropin (eCG). The ovaries were removed and transferred to M2 medium containing 0.2 mM 3-isobutyl-1-methylxanthine (IBMX; Nacalai Tesque, Kyoto, Japan). Ovarian follicles were punctured with a 26-G needle, and oocytes with homogenous cytoplasm were collected. The collected oocytes were grouped as follows: those with more than three layers of unexpanded cumulus cells (i.e., CEOs), those in which approximately half the cumulus layers were intact (partially denuded oocytes: PDOs), and those without cumulus cells (i.e., DOs). dCEOs and denuded PDOs (dPDOs) were prepared by mechanically removing cumulus cells from CEOs and PDOs using a narrow pipette, with pseudo-denuded DOs subjected to the same manipulation. CEOs, PDOs, and DOs are shown in Fig. 1.

Introduction of siRNA into GV-stage oocytes by electroporation

To perform the electroporation of oocytes, we employed the NEPA21 electroporator system (NEPA GENE, Chiba, Japan) with a glass slide and two metal electrodes separated by a 1-mm gap (CUY501P1-1.5; NEPA GENE). The electroporation parameters consisted of four poring pulses (40 V; pulse length, 1.0, 2.0, 3.0 or 4.0; interval, 50 msec; decay rate, 10%; polarity, +) and five transfer pulses (5 V; pulse length, 50 msec; interval, 50 msec; decay rate, 40%; polarity, +/−). Opti-MEM (Thermo Fisher Scientific, Waltham, MA, USA) containing siH3.3 (4 siRNAs at 5 µM each; RNAi Inc., Tokyo, Japan) or 4 µM red fluorescent non-targeting siRNA (BLOCK-iT™ Alexa Fluor® Red Fluorescent Control; Thermo Fisher Scientific) was prepared as the siRNA solution. The prepared siRNA solution (5 µl) was applied between the two electrodes on a glass slide. Oocytes were aligned between the electrodes, followed by the application of electrical discharge. The siRNA solution was exchanged every two operations to avoid dilution. After electroporation, oocytes were transferred to α-MEM supplemented with 5% fetal bovine serum and 10 ng/ml epidermal growth factor to induce meiotic maturation. *H3f3a* and *H3f3b* were targeted using the following siRNA sequences, as previously reported [29]: si*H3f3a* 1s, CGUUCAUUUGUGUGUGAAUUUtt; si*H3f3a* 1as, AAAUUCACACACAAAUGAACGtt; si*H3f3a* 2s, GCGAGAAAUUGCUCAGGACUUtt; si*H3f3a* 2as, AAGUCCUGAGCAAUUUCUCGCtt; si*H3f3b* 1s, UCUGAGAGAGAUCCGUCGUUAtt; si*H3f3b* 1as, UAACGACGGAUCUCUCUCAGAtt; si*H3f3b* 2s, GAAGCUGCCAUUCCAGAGAUUtt; and si*H3f3b* 2as, AAUCUCUGGAAUGGCAGCUUCtt. The following were also used: control siRNAs, UACGAAUGACGUGCGGUACGU; and control siRNA as, GUACCGCACGUCAUUCGUAUC.

In vitro fertilization (IVF) and embryo culture

After *in vitro* maturation (IVM) for 15–18 h, MII oocytes were transferred into a 100-µl droplet of human tubal fluid (HTF) medium supplemented with 4 mg/ml bovine serum albumin (BSA; Sigma-Aldrich, St. Louis, MO, USA) [31]. Spermatozoa were collected from the cauda epididymis of 12–18-week-old ICR male mice. After 1-h of preincubation in HTF medium, the sperm suspension was added to the fertilization droplets at a final concentration of 1×10^6 cells/ml. Six hours post-insemination (hpi), fertilized embryos were washed in potassium simplex optimized medium (KSOM) supplemented with amino acids [32] and 1 mg/ml BSA and then cultured in the same medium under paraffin oil (Nacalai Tesque). All incubations were performed at 37°C under 5% CO_2.

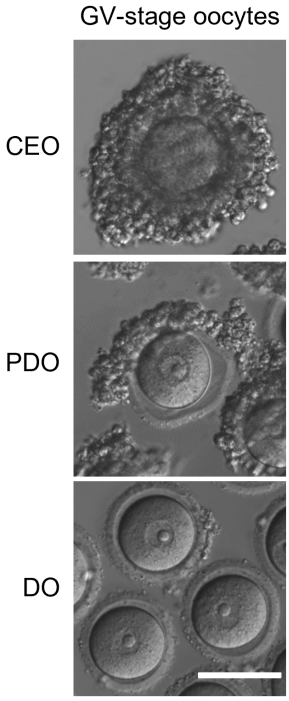

Fig. 1. Morphology of germinal vesicle (GV)-stage oocytes collected from mouse ovaries. Scale bar, 100 µm. CEO, cumulus-enclosed oocytes; DO, denuded oocytes; PDOs, partially denuded oocytes.

RNA extraction and reverse transcription-quantitative PCR (RT-qPCR)

Total RNA extraction and cDNA synthesis from oocytes or cumulus cells were performed using the superPrep™ Cell Lysis & RT Kit for qPCR (TOYOBO, Osaka, Japan). Synthesized cDNA was mixed with specific primers and KOD SYBR qPCR Mix (TOYOBO), followed by RT-qPCR amplification. The protocols for RT-qPCR and establishment of transcript levels were performed as previously described [33], and *Gapdh* was used as an internal control. The relative gene expression was calculated using the $2^{-\Delta\Delta Ct}$ method [34]. Primer sequences used for RT-qPCR were as follows: *Gapdh*, 5′-GTGTTCCTACCCCCAATGTG-3′ (forward) and 5′-TGTCATCATACTTGGCAGGTTTC-3′ (reverse); *H3f3a*, 5′-ACAAAAGCCGCTCGCAAGAG-3′ (forward) and 5′-ATTTCTCGCACCAGACGCTG-3′ (reverse); *H3f3b*, 5′-TGGCTCTGAGAGAGATCCGTCGTT-3′ (forward) and 5′-GGATGTCTTTGGGCATGATGGTGAC-3′ (reverse).

Immunocytochemistry and fluorescence analysis

To detect the nuclear localization of H3.3, oocytes and embryos were fixed with 3.2% paraformaldehyde and 0.2% Triton X-100 (Sigma-Aldrich) in phosphate-buffered saline (PBS) for 20 min at 28°C. Oocytes and embryos were blocked in PBS containing 1.5% BSA, 0.2% sodium azide, and 0.02% Tween20 (antibody dilution buffer) for 1 h at 28°C, followed by overnight incubation at 4°C

with rat anti-H3.3 (1:100) (CE-040B; Cosmo Bio, Tokyo, Japan) antibody in antibody dilution buffer. Subsequently, the samples were washed in antibody dilution buffer and incubated with Alexa Fluor 555 donkey anti-rat IgG secondary antibody (1:500; Thermo Fisher Scientific) for 1 h at 28°C. After washing in antibody dilution buffer, nuclei were stained with antibody dilution buffer containing 10 µg/ml Hoechst 33342 (Sigma-Aldrich) for 20 min at 28°C. Stained samples were mounted on glass slides, and signals were observed using a fluorescence microscope (IX73; Olympus, Tokyo, Japan). Hoechst staining revealed that the larger pronucleus located farther from the polar body was a male pronucleus. Similarly, GV-stage oocytes were mounted on glass slides, and fluorescence signals of BLOCK-iT™ Alexa Fluor® Red Fluorescent Control (Thermo Fisher Scientific) were observed using a fluorescence microscope (BX50; Olympus).

Statistical analyses

Developmental rates were analyzed using the chi-squared test with Holm's adjustment. For gene expression analysis, RT-qPCR data were analyzed using Student's *t*-test for pairwise comparisons or one-way analysis of variance (ANOVA) followed by the Tukey-Kramer test for multiple comparisons. P values < 0.05 were considered statistically significant.

Ethical approval for the use of animals

All experimental procedures were approved by the Animal Research Committee of Kyoto University (Permit no. R3-17) and performed in accordance with the committee's guidelines.

Results

The presence of cumulus cells affects the developmental competence of mouse GV-stage oocytes

The method used for introducing siRNA into mouse GV-stage oocytes was first investigated by examining differences in the developmental competence of each GV oocyte depending on the cumulus cell status. Three types of GV-stage oocytes were harvested from mouse ovaries: CEOs, PDOs, and DOs. In the first experiment, the three cell types were subjected to IVM and subsequent IVF to determine differences in fertilization and developmental rates. At 6 hpi, embryos with two pronuclei were defined as fertilized. Although there were no differences between fertilization rates, development to the blastocyst stage occurred at a significantly lower rate in DOs than that in CEOs (Table 1), which is consistent with previous reports [17, 18, 35]. In the next experiment, we compared the differences in the fertilization and developmental rates of CEOs, PDOs, and DOs with those of dCEOs and dPDOs. Denudation was performed using a pipette. Pseudo-denuded DOs were assessed to confirm the effects of the pipetting procedure on cumulus cell denudation; there was no difference in fertilization or developmental rate between DOs and pseudo-denuded DOs (data not shown). To further determine the effects of denudation and absence of cumulus cells on fertilization and subsequent development, the removed cumulus cells were co-cultured with dCEOs and DOs during IVM and IVF. The fertilization rates of dCEOs and dPDOs were dramatically reduced; this rate partially recovered when dCEOs were co-cultured with cumulus cells and developed into blastocysts (Table 1). Co-culture with cumulus cells did not impact the fertilization or developmental rates of DOs.

Assessing the electroporation of GV-stage oocytes using red fluorescent non-targeting siRNA

CEOs and DOs were subjected to electroporation to introduce siRNA into GV-stage oocytes without removing cumulus cells. To visualize the incorporation of siRNA into GV-stage oocytes, a red fluorescent non-targeting siRNA (BLOCK-iT™ Alexa Fluor® Red Fluorescent Control; Thermo Fisher Scientific) was introduced into CEOs and DOs by electroporation under various pulse conditions (pulse length:0, 1.0, 2.0, 3.0, and 4.0 msec). Under the longer pulse length, we confirmed that siRNA was more efficiently incorporated into GV-stage oocytes (Fig. 2).

The electroporation of siH3.3 effectively reduces the mRNA level of MII oocytes

To determine the efficacy of electroporation for suppressing specific genes, siRNAs targeting *H3f3a* and *H3f3b*, which encode histone H3.3, were introduced into GV-stage oocytes by electroporation (two siRNAs per gene, a total of four). Given that electroporation facilitated the more efficient incorporation of siRNA into GV-stage oocytes under longer pulse lengths, we further investigated whether the knockdown efficiency varied at pulse lengths of 1.0 or 4.0 msec. Immediately after electroporation, IVM was performed for 15 h, and the efficacy of suppressing gene expression was examined by RT-qPCR using oocytes that reached the MII stage. The expression of both *H3f3a* and *H3f3b* was suppressed by > 70% when compared with that of control cells electroporated with siControl, a non–gene targeting siRNA (Fig. 3A). The 1.0 and 4.0-msec pulse lengths resulted in comparable knockdown efficacy. Given that electroporation in zygotes under longer pulse length causes greater damage to zygotes [36] and that pulse length (1.0 and 4.0 msec) did not alter KD efficiency, a 1.0-msec pulse length was selected as the optimal condition. Gene expression was also suppressed in cumulus cells attached to CEOs,

Table 1. Effects of attached cumulus cells on developmental competence of CEOs, PDOs, and DOs

Oocyte	No. of GV-stage oocytes	No. (%) of embryos with two pronuclei	No. (%) of 2-cell embryos	No. (%) of blastocysts	% of blastocysts per fertilized embryo
CEO	103	67 (65.0) [a]	66 (64.1) [a]	56 (54.4) [a]	83.6 [a]
dCEO	102	3 (2.94) [c]	3 (2.94) [d]	0 (0.0) [d]	0.0 [ab]
dCEO + cumulus cells	59	12 (20.3) [b]	13 (22.0) [c]	10 (16.9) [c]	83.3 [ab]
PDO	98	70 (71.4) [a]	68 (69.4) [a]	42 (42.9) [ab]	60.0 [ab]
dPDO	117	44 (37.6) [b]	38 (32.5) [bc]	19 (16.2) [c]	43.2 [b]
DO	117	69 (59.0) [a]	58 (49.6) [ab]	36 (30.8) [bc]	52.2 [b]
DO + cumulus cells	104	70 (67.3) [a]	62 (59.6) [a]	49 (47.1) [ab]	70.0 [ab]

CEOs, cumulus-enclosed oocytes; DOs, denuded oocytes; dCEOs, denuded CEOs; dPDOs, denuded PDOs; GV, germinal vesicle; PDOs, partially denuded oocytes. Different letters in the same column (a, b, c, and d) represent significant differences (P-value < 0.05).

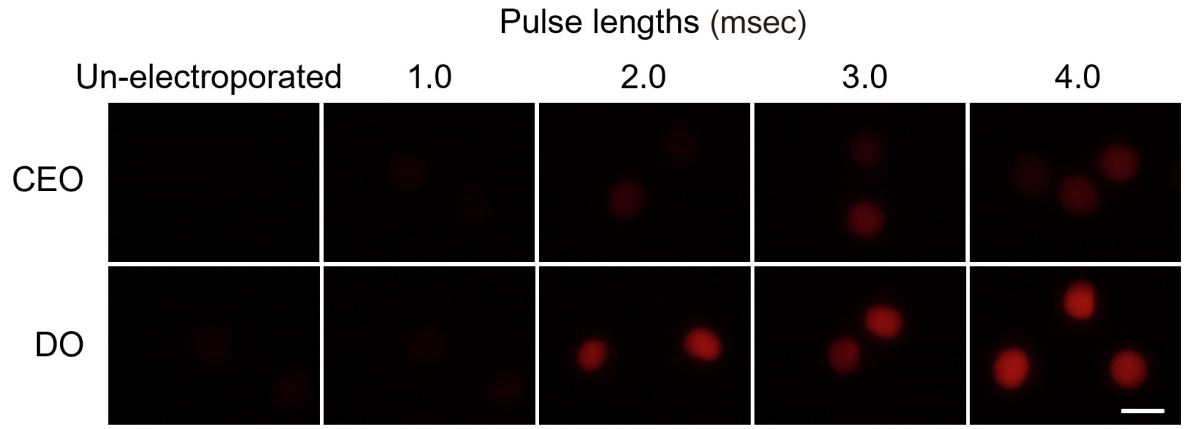

Fig. 2. Effects of pulse length on siRNA incorporation into cumulus-enclosed oocytes (CEOs) and denuded oocytes (DOs). Representative images of CEOs (un-electroporated, n = 12; 1.0 msec, n = 9; 2.0 msec, n = 12; 3.0 msec, n = 11; and 4.0 msec, n = 13) and DOs (un-electroporated, n = 10; 1.0 msec, n = 11; 2.0 msec, n = 10; 3.0 msec, n = 12; and 4.0 msec, n = 12) electroporated with red fluorescent non-targeting siRNA under various pulse lengths are shown. Scale bar, 100 μm.

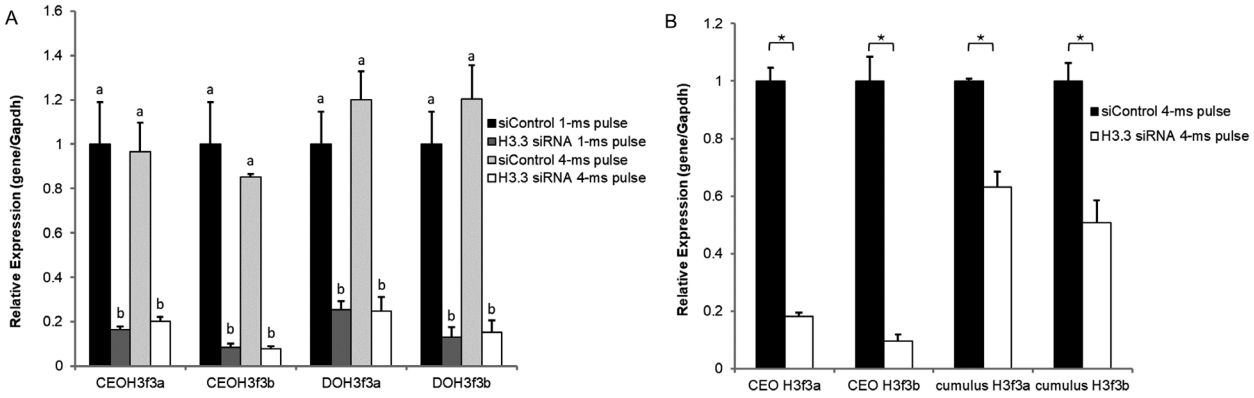

Fig. 3. Reverse transcription-quantitative PCR (RT-qPCR) analysis of *H3f3a* and *H3f3b* mRNA in H3.3-knockdown oocytes at the metaphase II (MII) stage. (A) RT-qPCR of *H3f3a* and *H3f3b* was performed using electroporated cumulus-enclosed oocytes (CEOs) and denuded oocytes (DOs) after *in vitro* maturation (IVM). Gene expression levels were normalized to *Gapdh* as an internal control. Data are expressed as means ± standard error of the mean (S.E.M) (n = 3). In total, 11–15 embryos were analyzed. Statistical analysis was performed using one-way analysis of variance (ANOVA) followed by the Tukey-Kramer test. P values < 0.05 were considered statistically significant and are represented by different letters (a and b). (B) RT-qPCR of *H3f3a* and *H3f3b* was performed using cumulus cells attached to electroporated CEOs after IVM. Gene expression levels were normalized to *Gapdh* as an internal control. Data are expressed as means ± S.E.M (n = 3). Statistical analysis was performed using Student's *t*-test. P values < 0.05 were considered statistically significant.

suggesting that siRNA was introduced into cumulus cells (Fig. 3B).

H3.3 is incorporated into the nucleus of GV-stage oocytes, and its incorporation into the paternal pronucleus can be blocked after fertilization

To monitor the expression of H3.3 (before and after fertilization) and confirm reduced H3.3 protein expression induced by siRNA treatment, we performed immunofluorescence staining for H3.3 from the GV stage to the one-cell stage. H3.3 was previously incorporated into the nuclei of GV-stage oocytes (Fig. 4A). In MII oocytes, H3.3 was incorporated into the nucleosomes of both control and H3.3 knockdown oocytes (Fig. 4B). At 6 hpi, H3.3 was incorporated into maternal and paternal pronuclei and nuclei of two polar bodies in control embryos. In contrast, H3.3 was not incorporated into the paternal pronuclei of H3.3 knockdown embryos (Fig. 4B). H3.3 is present in the oocyte as a maternal factor and undergoes incorporation into the paternal pronucleus immediately after fertilization. However, it remains unclear how maternal H3.3 removal from GV-stage oocytes affects post-fertilization development [23, 24, 37]. CEOs and DOs electroporated with siH3.3 or siControl with a 1.0-msec pulse length were subjected to IVM for 15 h to examine maturation rates and the differences in fertilization and developmental rates after IVF (Table 2). Herein, we observed that siH3.3 did not impact maturation or fertilization rates, although the rate of development to the two-cell stage was markedly reduced (Fig. 4C and Table 2). Compared with oocytes that did not undergo electroporation, oocytes electroporated with siControl exhibited no decrease in maturation, fertilization, or developmental rates.

Discussion

The findings of the present study revealed the reduced developmental competence of DOs after fertilization, consistent with those reported previously [17, 18, 35]. DOs exhibit a higher proportion of oocytes with non-surrounded nuclear (NSN)-type chromatin configurations than CEOs [3, 17]. NSN-type oocytes are often unable

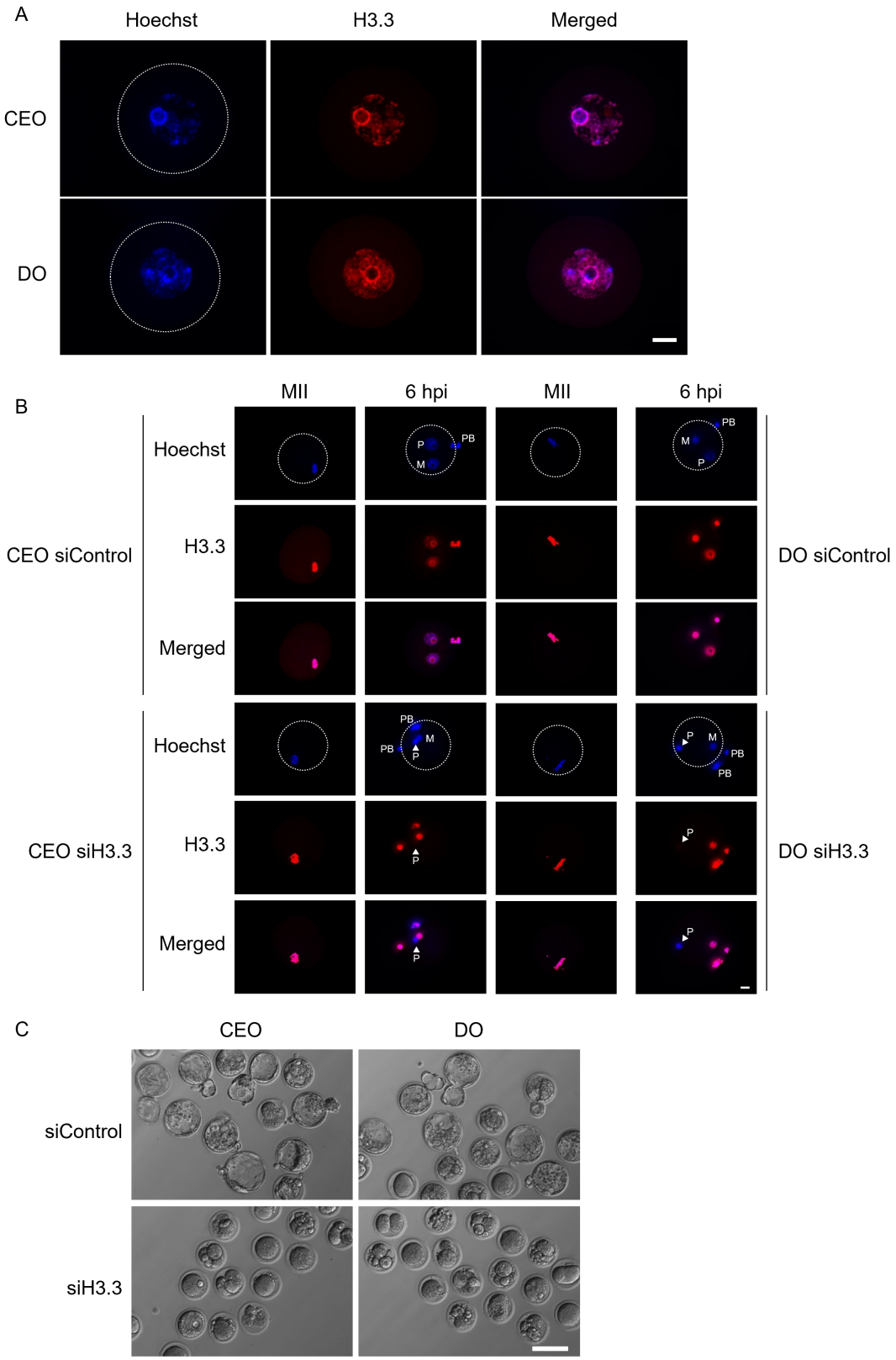

Fig. 4. Effects of si*H3.3* treatment on H3.3 incorporation into germinal vesicle (GV)-stage oocytes before and after fertilization. Oocytes and embryos were stained with anti-H3.3 antibody. (A) Localization of H3.3 in cumulus-enclosed oocytes (CEOs) (n = 27) and denuded oocytes (DOs) (n = 18). The cumulus cells of CEOs were removed for immunostaining. H3.3 is present in the nuclei of GV-stage oocytes and cumulus cells. Scale bar, 20 µm. (B) Localization of H3.3 in metaphase II (MII) oocytes (CEO siControl, n = 11; CEO siH3.3, n = 16; DO siControl, n = 7; and DO siH3.3, n = 7) and one-cell embryos (CEO siControl, n = 11; CEO siH3.3, n = 15; DO siControl, n = 9; and DO siH3.3, n = 16). H3.3 is localized in the nuclei of MII oocytes treated with or without siH3.3. However, H3.3 is not localized in the paternal pronuclei of embryos at 6 h post-insemination (hpi) produced after treatment with si*H3.3* at the GV stage. Scale bar, 20 µm. (C) Developmental competence of embryos electroporated with siH3.3 at the germinal vesicle (GV) stage. Representative images of embryos electroporated with either si*H3.3* or siControl at the GV stage. Embryos were photographed at 96 hpi. Scale bar, 100 µm.

Table 2. Effects of electroporation of si*H3.3* on the developmental competence of CEOs and DOs

Treatment of GV oocytes	No. of GV-stage oocytes	No. (%) of MII-stage oocytes	No. (%) of embryos with two pronuclei	No. (%) of 2-cell embryos	No. (%) of 4-cell embryos	No. (%) of morulae	No. (%) of blastocysts	% of blastocysts per fertilized embryo
Un-electroporated CEO	60	58 (96.7) [a]	31 (51.7) [a]	27 (45.0) [a]	24 (40.0) [a]	25 (41.7) [a]	24 (40.0) [a]	77.4 [a]
siControl CEO	64	64 (100.0) [a]	23 (35.9) [a]	23 (35.9) [a]	20 (31.3) [a]	18 (28.1) [a]	15 (23.4) [a]	65.2 [a]
siH3.3 CEO	64	64 (100.0) [a]	24 (37.5) [a]	4 (6.2) [b]	1 (1.5) [b]	0 (0.0) [b]	0 (0.0) [b]	0.0 [b]
Un-electroporated DO	60	57 (95.0) [a]	24 (40.0) [a]	23 (38.3) [a]	18 (30.0) [a]	16 (26.7) [a]	13 (21.7) [a]	54.2 [a]
siControl DO	63	61 (96.8) [a]	26 (41.3) [a]	23 (36.5) [a]	23 (36.5) [a]	20 (31.7) [a]	16 (25.4) [a]	61.5 [a]
siH3.3 DO	55	54 (98.2) [a]	28 (50.9) [a]	7 (12.7) [b]	1 (1.8) [b]	0 (0.0) [b]	0 (0.0) [b]	0.0 [b]

CEOs, cumulus-enclosed oocytes; DOs, denuded oocytes; GV, germinal vesicle. Different letters (a and b) in the same column represent significant differences (P-value < 0.05).

to complete meiosis, and the reduced developmental competence of DOs may be attributed to the predominance of these oocytes [38, 39]. It can be suggested that DOs are generated by the apoptosis of granulosa and cumulus cells during folliculogenesis, a phenomenon called atresia [19, 40, 41]. This process may disrupt the transzonal cytoplasmic processes between oocytes and cumulus cells, thus reducing the supply of factors, such as cAMP, which control oocyte maturation and decrease DO quality [42]. Our results showed that dCEOs had markedly lower fertilization competence than CEOs. Considering dCEOs, distinct fertilization and developmental rates have been reported [43–47], which may be attributed to differences between mouse strains, culture media, and the extent of cumulus cell removal. Herein, we revealed that the addition of cumulus cells to dCEOs partially restored fertilization and developmental rates, supporting the importance of oocyte-cumulus cell communication [42] and suggesting that dCEOs can be effectively used with this method. These results indicate that, when studying post-fertilization developmental rates, CEOs mimic *in vivo* conditions more accurately than DOs or dCEOs.

We found that electroporation can introduce siRNA into CEOs and DOs, thereby suppressing target genes. However, in the case of CEO electroporation, siRNAs were also introduced into cumulus cells; thus, caution should be exercised when targeting genes expressed in cumulus cells. Although a higher incorporation rate was observed with longer pulse lengths, the knockdown efficacy was independent of pulse length, suggesting that a sufficient amount of siRNA can be introduced for gene knockdown in mouse preimplantation embryos, regardless of pulse length. Only one study has examined the mechanisms of embryo development using antisense oligonucleotide injections at the GV stage, followed by IVF [48]. This could be attributed to the use of DOs and dCEOs with extremely low fertilization and developmental competence; therefore, acquiring sufficient fertilized eggs for analysis can be challenging. Using the electroporation method, we could introduce siH3.3 into DOs and CEOs and evaluate the impact of H3.3 on developmental competence after fertilization. Compared with the electroporation of DOs, electroporation of CEOs resulted in low levels of siRNA introduction, possibly due to surrounding cumulus cells. It has been reported that H3.3 is preferentially incorporated into the paternal pronucleus, and H3.3 knockdown in GV-stage oocytes can induce abnormal pronuclear formation [13]. Our results showed that H3.3 was already present in GV-stage oocytes, as previously reported [24, 49]. In addition, H3.3 localization in the maternal pronucleus was unaltered following the introduction of siH3.3, suggesting that H3.3 incorporated into the maternal genome is tightly bound to the genome, even during the transition from GV to MII. In addition, siH3.3 electroporation into GV-stage oocytes inhibited H3.3 incorporation into the paternal pronucleus after fertilization, indicating that maternal H3.3 protein is repeatedly translated and degraded in the oocyte and that siH3.3-mediated depletion of H3.3 mRNA causes a gradual decrease in H3.3 protein during oocyte maturation. Furthermore, electroporating GV-stage oocytes with siH3.3 reduced developmental competence after fertilization, revealing that incorporating H3.3 into the paternal pronucleus is required for subsequent embryonic development.

The method of electroporating siRNA into GV-stage oocytes, as described in the present study, is a powerful tool to analyze the function of maternal factors and establish the involvement of these factors in embryonic development after fertilization. This method may also apply to genome editing involving the introduction of guide RNA and Cas9 protein, potentially allowing the generation of maternal allele-specific knockout mice. In summary, we comprehensively analyzed the fertility and developmental competence of CEOs, DOs, and dCEOs. Moreover, we established an electroporation method for introducing siRNA into CEOs to genetically analyze fully grown oocytes without compromising their developmental potential.

Conflict of interests: The authors declare that there are no conflicts of interest that might be perceived as prejudicing the impartiality of the reported research.

Acknowledgments

This work was supported by Grant-in-Aid for Scientific Research (no. 19H03136 to NM) and Grant-in-Aid for JSPS Fellows (no. 21J21840 to TY) from the Japan Society for the Promotion of Science.

References

1. **Bachvarova R.** Gene expression during oogenesis and oocyte development in mammals. *Dev Biol (N Y 1985)* 1985; **1**: 453–524. [Medline]
2. **Aoki F, Worrad DM, Schultz RM.** Regulation of transcriptional activity during the first and second cell cycles in the preimplantation mouse embryo. *Dev Biol* 1997; **181**: 296–307. [Medline] [CrossRef]
3. **De La Fuente R, Eppig JJ.** Transcriptional activity of the mouse oocyte genome: companion granulosa cells modulate transcription and chromatin remodeling. *Dev Biol* 2001; **229**: 224–236. [Medline] [CrossRef]
4. **Minami N, Suzuki T, Tsukamoto S.** Zygotic gene activation and maternal factors in mammals. *J Reprod Dev* 2007; **53**: 707–715. [Medline] [CrossRef]
5. **Miyamoto K.** Maternal factors involved in nuclear reprogramming by eggs and oocytes. *J Mamm Ova Res* 2013; **30**: 68–78. [CrossRef]
6. **Zhang K, Smith G.** Maternal control of early embryogenesis in mammals. *Reprod Fertil Dev* 2015; **27**: 880–896.
7. **Tadros W, Lipshitz HD.** The maternal-to-zygotic transition: a play in two acts. *Development* 2009; **136**: 3033–3042. [Medline] [CrossRef]

8. **Tong Z-B, Gold L, Pfeifer KE, Dorward H, Lee E, Bondy CA, Dean J, Nelson LM.** Mater, a maternal effect gene required for early embryonic development in mice. *Nat Genet* 2000; **26**: 267–268. [Medline] [CrossRef]
9. **Wu X, Viveiros MM, Eppig JJ, Bai Y, Fitzpatrick SL, Matzuk MM.** Zygote arrest 1 (Zar1) is a novel maternal-effect gene critical for the oocyte-to-embryo transition. *Nat Genet* 2003; **33**: 187–191. [Medline] [CrossRef]
10. **Rajkovic A, Pangas SA, Ballow D, Suzumori N, Matzuk MM.** NOBOX deficiency disrupts early folliculogenesis and oocyte-specific gene expression. *Science* 2004; **305**: 1157–1159. [Medline] [CrossRef]
11. **Honda S, Miki Y, Miyamoto Y, Kawahara Y, Tsukamoto S, Imai H, Minami N.** Oocyte-specific gene Oog1 suppresses the expression of spermatogenesis-specific genes in oocytes. *J Reprod Dev* 2018; **64**: 297–301. [Medline] [CrossRef]
12. **Inoue A, Matoba S, Zhang Y.** Transcriptional activation of transposable elements in mouse zygotes is independent of Tet3-mediated 5-methylcytosine oxidation. *Cell Res* 2012; **22**: 1640–1649. [Medline] [CrossRef]
13. **Inoue A, Zhang Y.** Nucleosome assembly is required for nuclear pore complex assembly in mouse zygotes. *Nat Struct Mol Biol* 2014; **21**: 609–616. [Medline] [CrossRef]
14. **Peng H, Wu Y, Zhang Y.** Efficient delivery of DNA and morpholinos into mouse preimplantation embryos by electroporation. *PLoS One* 2012; **7**: e43748. [Medline] [CrossRef]
15. **Kaneko T, Sakuma T, Yamamoto T, Mashimo T.** Simple knockout by electroporation of engineered endonucleases into intact rat embryos. *Sci Rep* 2014; **4**: 6382. [Medline] [CrossRef]
16. **Peng H, Chang B, Lu C, Su J, Wu Y, Lv P, Wang Y, Liu J, Zhang B, Quan F, Guo Z, Zhang Y.** Nlrp2, a maternal effect gene required for early embryonic development in the mouse. *PLoS One* 2012; **7**: e30344. [Medline] [CrossRef]
17. **Liu H, Aoki F.** Transcriptional activity associated with meiotic competence in fully grown mouse GV oocytes. *Zygote* 2002; **10**: 327–332. [Medline] [CrossRef]
18. **Kikuchi H, Yoshizawa M, Tanemura K, Sato E, Yoshida H.** Risk of premature chromatid separation is increased by poor cumulus cell layers and inappropriate culture media for in vitro maturation of mouse oocytes. *J Mamm Ova Res* 2016; **33**: 63–68. [CrossRef]
19. **Gougeon A, Testart J.** Germinal vesicle breakdown in oocytes of human atretic follicles during the menstrual cycle. *J Reprod Fertil* 1986; **78**: 389–401. [Medline] [CrossRef]
20. **Lefèvre B, Gougeon A, Peronny H, Testart J.** Effect of cumulus cell mass and follicle quality on in-vitro maturation of cynomolgus monkey oocytes. *Hum Reprod* 1988; **3**: 891–893. [Medline] [CrossRef]
21. **Blondin P, Sirard M-A.** Oocyte and follicular morphology as determining characteristics for developmental competence in bovine oocytes. *Mol Reprod Dev* 1995; **41**: 54–62. [Medline] [CrossRef]
22. **Hinrichs K, Williams KA.** Relationships among oocyte-cumulus morphology, follicular atresia, initial chromatin configuration, and oocyte meiotic competence in the horse. *Biol Reprod* 1997; **57**: 377–384. [Medline] [CrossRef]
23. **Torres-Padilla M-E, Bannister AJ, Hurd PJ, Kouzarides T, Zernicka-Goetz M.** Dynamic distribution of the replacement histone variant H3.3 in the mouse oocyte and preimplantation embryos. *Int J Dev Biol* 2006; **50**: 455–461. [Medline] [CrossRef]
24. **Akiyama T, Suzuki O, Matsuda J, Aoki F.** Dynamic replacement of histone H3 variants reprograms epigenetic marks in early mouse embryos. *PLoS Genet* 2011; **7**: e1002279. [Medline] [CrossRef]
25. **Lin C-J, Conti M, Ramalho-Santos M.** Histone variant H3.3 maintains a decondensed chromatin state essential for mouse preimplantation development. *Development* 2013; **140**: 3624–3634. [Medline] [CrossRef]
26. **Lin C-J, Koh FM, Wong P, Conti M, Ramalho-Santos M.** Hira-mediated H3.3 incorporation is required for DNA replication and ribosomal RNA transcription in the mouse zygote. *Dev Cell* 2014; **30**: 268–279. [Medline] [CrossRef]
27. **Ishiuchi T, Abe S, Inoue K, Yeung WKA, Miki Y, Ogura A, Sasaki H.** Reprogramming of the histone H3.3 landscape in the early mouse embryo. *Nat Struct Mol Biol* 2021; **28**: 38–49. [Medline] [CrossRef]
28. **Aoki F.** Zygotic gene activation in mice: profile and regulation. *J Reprod Dev* 2022; **68**: 79–84. [Medline] [CrossRef]
29. **Wen D, Banaszynski LA, Liu Y, Geng F, Noh KM, Xiang J, Elemento O, Rosenwaks Z, Allis CD, Rafii S.** Histone variant H3.3 is an essential maternal factor for oocyte reprogramming. *Proc Natl Acad Sci USA* 2014; **111**: 7325–7330. [Medline] [CrossRef]
30. **Kong Q, Banaszynski LA, Geng F, Zhang X, Zhang J, Zhang H, O'Neill CL, Yan P, Liu Z, Shido K, Palermo GD, Allis CD, Rafii S, Rosenwaks Z, Wen D.** Histone variant H3.3-mediated chromatin remodeling is essential for paternal genome activation in mouse preimplantation embryos. *J Biol Chem* 2018; **293**: 3829–3838. [Medline] [CrossRef]
31. **Minami N, Sasaki K, Aizawa A, Miyamoto M, Imai H.** Analysis of gene expression in mouse 2-cell embryos using fluorescein differential display: comparison of culture environments. *Biol Reprod* 2001; **64**: 30–35. [Medline] [CrossRef]
32. **Ho Y, Wigglesworth K, Eppig JJ, Schultz RM.** Preimplantation development of mouse embryos in KSOM: augmentation by amino acids and analysis of gene expression. *Mol Reprod Dev* 1995; **41**: 232–238. [Medline] [CrossRef]
33. **Shikata D, Yamamoto T, Honda S, Ikeda S, Minami N.** H4K20 monomethylation inhibition causes loss of genomic integrity in mouse preimplantation embryos. *J Reprod Dev* 2020; **66**: 411–419. [Medline] [CrossRef]
34. **Livak KJ, Schmittgen TD.** Analysis of relative gene expression data using real-time quantitative PCR and the 2(-Δ Δ C(T)) method. *Methods* 2001; **25**: 402–408. [Medline] [CrossRef]
35. **Shioya Y, Kuwayama M, Fukushima M, Iwasaki S, Hanada A.** In vitro fertilization and cleavage capability of bovine follicular oocytes classified by cumulus cells and matured in vitro. *Theriogenology* 1988; **30**: 489–496. [Medline] [CrossRef]
36. **Chen S, Lee B, Lee AYF, Modzelewski AJ, He L.** Highly efficient mouse genome editing by CRISPR ribonucleoprotein electroporation of zygotes. *J Biol Chem* 2016; **291**: 14457–14467. [Medline] [CrossRef]
37. **van der Heijden GW, Dieker JW, Derijck AAHA, Muller S, Berden JHM, Braat DDM, van der Vlag J, de Boer P.** Asymmetry in histone H3 variants and lysine methylation between paternal and maternal chromatin of the early mouse zygote. *Mech Dev* 2005; **122**: 1008–1022. [Medline] [CrossRef]
38. **Debey P, Szöllösi MS, Szöllösi D, Vautier D, Girousse A, Besombes D.** Competent mouse oocytes isolated from antral follicles exhibit different chromatin organization and follow different maturation dynamics. *Mol Reprod Dev* 1993; **36**: 59–74. [Medline] [CrossRef]
39. **Zuccotti M, Ponce RH, Boiani M, Guizzardi S, Govoni P, Scandroglio R, Garagna S, Redi CA.** The analysis of chromatin organisation allows selection of mouse antral oocytes competent for development to blastocyst. *Zygote* 2002; **10**: 73–78. [Medline] [CrossRef]
40. **Osman P.** Rate and course of atresia during follicular development in the adult cyclic rat. *J Reprod Fertil* 1985; **73**: 261–270. [Medline] [CrossRef]
41. **Hirshfield AN.** Development of follicles in the mammalian ovary. *Int Rev Cytol* 1991; **124**: 43–101. [Medline] [CrossRef]
42. **Sutton ML, Gilchrist RB, Thompson JG.** Effects of in-vivo and in-vitro environments on the metabolism of the cumulus-oocyte complex and its influence on oocyte developmental capacity. *Hum Reprod Update* 2003; **9**: 35–48. [Medline] [CrossRef]
43. **Schroeder AC, Eppig JJ.** The developmental capacity of mouse oocytes that matured spontaneously in vitro is normal. *Dev Biol* 1984; **102**: 493–497. [Medline] [CrossRef]
44. **Chang HC, Liu H, Zhang J, Grifo J, Krey LC.** Developmental incompetency of denuded mouse oocytes undergoing maturation in vitro is ooplasmic in nature and is associated with aberrant Oct-4 expression. *Hum Reprod* 2005; **20**: 1958–1968. [Medline] [CrossRef]
45. **Miki H, Ogonuki N, Inoue K, Baba T, Ogura A.** Improvement of cumulus-free oocyte maturation in vitro and its application to microinsemination with primary spermatocytes in mice. *J Reprod Dev* 2006; **52**: 239–248. [Medline] [CrossRef]
46. **Mahmodi R, Abbasi M, Amiri I, Kashani IR, Pasbakhsh P, Saadipour K, Amidi F, Abolhasani F, Sobhani A.** Cumulus cell role on mouse germinal vesicle oocyte maturation, fertilization, and subsequent embryo development to blastocyst stage in vitro. *Yakhteh* 2009; **11**: 299–302.
47. **Zhou C-J, Wu S-N, Shen J-P, Wang D-H, Kong X-W, Lu A, Li Y-J, Zhou H-X, Zhao Y-F, Liang C-G.** The beneficial effects of cumulus cells and oocyte-cumulus cell gap junctions depends on oocyte maturation and fertilization methods in mice. *PeerJ* 2016; **4**: e1761. [Medline] [CrossRef]
48. **Arand J, Chiang HR, Martin D, Snyder MP, Sage J, Reijo Pera RA, Wossidlo M.** Tet enzymes are essential for early embryogenesis and completion of embryonic genome activation. *EMBO Rep* 2022; **23**: e53968. [Medline] [CrossRef]
49. **Nashun B, Hill PWS, Smallwood SA, Dharmalingam G, Amouroux R, Clark SJ, Sharma V, Ndjetehe E, Pelczar P, Festenstein RJ, Kelsey G, Hajkova P.** Continuous histone replacement by hira is essential for normal transcriptional regulation and de novo DNA Methylation during mouse oogenesis. *Mol Cell* 2015; **60**: 611–625. [Medline] [CrossRef]